Internal catalysis on the opposite side of the fence in non-isocyanate polyurethane covalent adaptable networks

Aitor Hernández, Hannes Houck, Fermin Elizalde, Marc Guerre, Haritz Sardon, Filip Du Prez

Internal catalysis on the opposite side of the fence in non-isocyanate polyurethane covalent adaptable networks

Aitor Hernández,[a] Hannes A. Houck,[a] Fermin Elizalde,[b] Marc Guerre,[c] Haritz Sardon [b]* and Filip E. Du Prez [a]**

[a] *Polymer Chemistry Research Group, Centre of Macromolecular Chemistry (CMaC), Department of Organic and Macromolecular Chemistry, Faculty of Sciences, Ghent University, Krijgslaan 281 S4-bis, Ghent B-9000, Belgium.*

[b] *POLYMAT, University of the Basque Country UPV/EHU, Joxe Mari Korta Center, Avda. Tolosa 7, 20018 Donostia-San Sebastian, Spain*

[c] *Laboratoire des IMRCP Université de Toulouse CNRS UMR5623 Université Paul Sabatier 118 route de Narbonne, Toulouse 31062 Cedex 9, France*

*Marc Guerre: guerre@chimie.ups-tlse.fr, *Haritz Sardon: haritz.sardon@ehu.eus, *Filip E. Du Prez: filip.duprez@ugent.be

Abstract

Within the context of covalent adaptable networks (CANs), we developed in this study a novel methodology to provide non-isocyanate polyurethane-based CANs with embedded tertiary amines that serve as internal catalytic moieties for the dynamic bond exchange processes. For the CAN design, we made use of multifunctional N-substituted 8-membered cyclic carbonates that are ring-opened by macromolecular amines. Several model reactions were conducted to investigate transcarbamoylation bond exchange reactions at elevated temperatures and assess the influence of catalytic moieties within the urethane structure. This led us to design a non-isocyanate polyurethane CAN wherein the position of the internal catalyst was changed with respect to previous reported polyhydroxyurethane CANs, while maintaining close proximity to the dynamic carbamate linkages. It is shown that this positioning change of the tertiary amines still resulted in an internal catalytic effect on the dynamic exchange reactions, hence providing a better understanding of the role of tertiary amines as internal catalysts during the reprocessing of polyurethane networks. Moreover, the model experiments and thermomechanical investigations of the (re)processed networks allowed to identify the occurrence of competing reactions, involving a dissociative mechanism giving rise to urea formation, which significantly impacts the materials' reprocessability and properties.

Keywords

Covalent adaptable network, non-isocyanate polyurethane, polyhydroxyurethane, transcarbamoylation, internal catalysis.

1. Introduction

The discovery of thermoplastics marked a scientific revolution in the field of material sciences because of their low viscosity when heated beyond their glass transition or melting temperature when compared to metal based materials, enabling processing operations such as extrusion and injection moulding.[1] However, thermoset materials proved to possess far superior mechanical properties[2] because of their crosslinked structure, making them attractive as high performance materials such as engineering-grade composites.[3] Yet, thermosetting materials lack thermo-mechanically induced reprocessability because of their permanent covalent network structure. Being the main drawback of conventional thermoset materials, Bowman and co-workers [4–6] broke new ground by introducing reversible covalent bonds within the network structure, thereby creating a new class of polymeric materials known as covalent adaptable networks (CANs). Unlike previously known non-covalent networks relying on supramolecular interactions,[7–9] CANs consist of chemically crosslinked polymers that display healing and original viscosity dependence when subjected to specific stimuli such as light,[10] pH change[11] or heat[12] as a result of dissociative and/or associative covalent bond exchange mechanisms.[13]

A specific subclass of associative CAN materials known as 'vitrimers', introduced by Leibler *et al.*,[14,15] exhibits a linear viscosity dependence that follows an Arrhenian behaviour. This means that the rheological profile is controlled by the thermally initiated associative exchange reactions, resulting in a steady change in viscosity while keeping their crosslink density unaltered.[16] This rheological behaviour allows for a specific viscosity control different than to thermo-responsive dissociative CANs that follow a Williams-Landen-Ferry model and typically lose their network connectivity as the temperature rises[16,17]. In addition to the original polyester-based vitrimers,[14,15] numerous other chemical platforms have been widely developed to yield new types of vitrimer materials.[13,16,18]. However, dissociative processes which do not induce a considerable loss in crosslink density, may have a negligible effect on the viscoelastic properties, allowing the network to still follow the aforementioned Arrhenian behaviour within a specific temperature interval.[17,19,20] Additionally, despite the clear distinction between associative and dissociative mechanisms, CANs in which both kinds of mechanisms coexist have been identified (e.g. those based on polyhydroxyurethane backbones). [19,21]

Often, different types of CANs have proven to be effective only when subjected to the presence of external catalysts,[15,22] which could be problematic in case the catalyst becomes deactivated, degrades upon reprocessing, or leaches out during the material's live cycle.[16] Additionally, the catalyst could influence the associative/dissociative nature of the involved chemical exchange reactions, e.g. organotin catalysts in carbamate exchanges.[23–25] Hence, dynamic systems which are free of external catalysts,[26–28] do not require any catalysts at all, or entail an internal catalyst that remains covalently attached within the material, have attracted considerable attention. In particular the latter is an interesting design principle. Indeed, the chemical environment is a key factor in understanding chemical reactivity as bond exchange processes are often influenced by the stereoelectronic effects in the vicinity of the reactive sites.[29] In this context, internally catalysed networks[30] should be highlighted where strong hydrogen bonding or covalent

interactions have been proven to highly impact several chemistry platforms, allowing some dynamic materials to display faster exchange rates.[31–34] This has been proven to be a tuneable characteristic by altering the entropy of activation through displacement of the functionality that induces the internal catalytic effect (e.g. neighbouring group participation in the phthalate monoester transesterification)[35,36] or by adding even more accumulative effects within the proximity of the dynamic bond (e.g. double neighbouring group participation).[37]

Polyurethane-based CANs are an interesting type of materials with regard to catalysed bond exchange processes[24,25]. In particular, so-called non-isocyanate polyurethanes (NIPUs)[38,39] are an emerging class of more sustainable dynamic PU-based networks, since NIPU building blocks can be potentially derived from renewable feedstock such as cyclic carbonates from CO_2 whereby toxic isocyanates can be avoided.[40,41] Whereas for many decades, polyurethanes (PUs) have been industrially relevant because of their versatility and wide range of properties – making them ideal for an array of applications ranging from foams to coatings[42] –, PUs gain increasing attention as they are often used in (self-)healable dynamic networks.[43] Indeed, many polyurethane materials exhibit dynamic properties owed to transcarbamoylation reactions that are externally catalysed by, e.g. organotin, organic acid or Lewis acid compounds, which are commonly used in their preparation.[23,44] Yet, metal-free dynamic polyurethane and polyhydroxyurethane (PHU) networks having tertiary amine moieties in the beta-position to the carbamate nitrogens (denoted as **R_3N_β-N** in Fig. 1.A, left) have also been reported.[45–50]

Given that tertiary amine-based external organocatalysts have been used as an alternative to tin catalysts in the design and depolymerisation process of PUs,[51,52] we hypothesized that the embedded amines might have an internal catalytic effect on the transcarbamoylation reaction. Since the spatial proximity of the amine would be a key factor as internal catalysis is governed by bond distance rather than at which side of the urethane linkage it is attached to, having tertiary amine moieties in the beta-position to the carbamate oxygen (**R_3N_β-O**, see Fig. 1.A, right) instead of the carbamate nitrogen **R_3N_β-N** should still result in transcarbamoylation exchange reactions.

To investigate our hypothesis, a series of small molecule experiments were performed to monitor both associative and dissociative bond exchanges of different carbamates, with and without the presence of a tertiary amine in the beta-position, at elevated temperatures. Further, we synthesised a new internally catalysed non-isocyanate polyurethane (IC-NIPU, Fig. 1.B) using N-substituted 8-membered cyclic carbonates, which in the presence of amines give rise to polyhydroxyurethanes wherein the tertiary amine moieties are not positioned in the beta-position relative to the carbamate nitrogen but are incorporated on the opposite, carbamate oxygen side (**R_3N_β-O**). The thermal and mechanical properties of the resulting networks were evaluated in terms of their reprocessability, which resulted in the identification of urea bond formation that competes with the dynamic transcarbamoylation reactions.

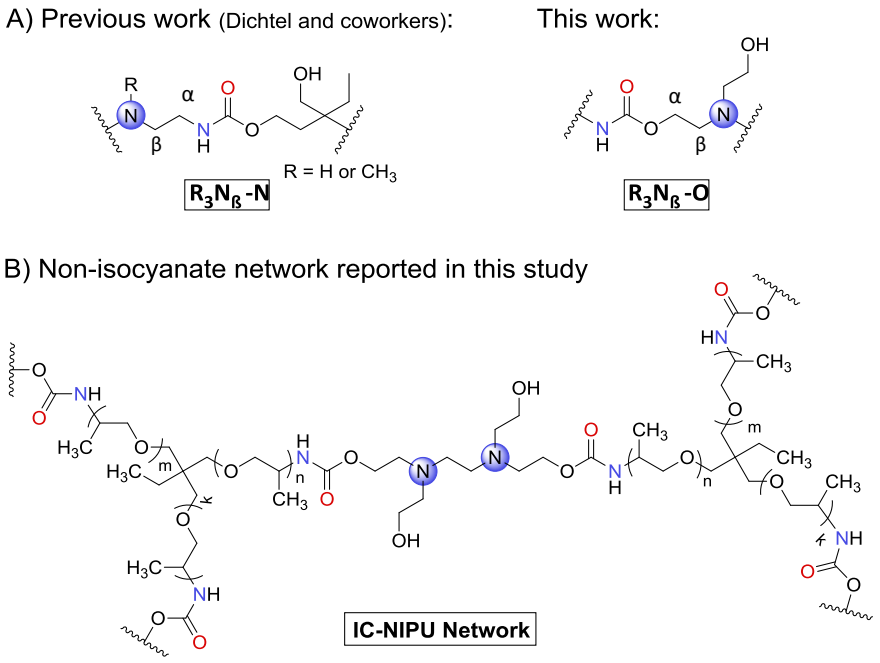

Fig. 1. A) Dynamic polyhydroxyurethane linkage based on tertiary amine moieties in beta position to the carbamate nitrogen (**R_3N_β-N**), as reported by Dichtel and co-workers (left),[45] and where the tertiary amine position is displaced towards the carbamate oxygen (**R_3N_β-O**) as investigated in this work. **B)** Synthesis of internally catalysed non-isocyanate polyurethane (**IC-NIPU**) covalent adaptable network.

2. Experimental Section

2.1 Reagents and Solvents

Bis(pentafluorophenyl)carbonate 97 % (Fluorochem CAS: 59483-84-0), butyl isocyanate 98 % (Sigma-Aldrich, CAS: 111-36-4), chloroform ≥99.8 % (Sigma-Aldrich, CAS: 67-66-3), chloroform-D_3 99.80 % D (Eurisotop, CAS:865-49-6), 2-cyclohexylethanol 99 % (Alfa Aesar, CAS: 4442-79-9), dibutyltin dilaurate >95.0 % (TCI Europe, CAS: 77-58-7), dichloromethane ≥99.8 % (Sigma-Aldrich, CAS: 75-09-2), 2-(diethylamino)-ethanol >99 % (Alfa Aesar, CAS: 100-37-8), diglycerol (mixture of isomers) >80.0 % (TCI Europe, CAS: 627-82-7), dimethyl carbonate 99 % (Sigma-Aldrich, CAS: 616-38-6), 2-(dimethylamino)-ethanol >99 % (Alfa Aesar, CAS: 108-01-0), dimethylsufoxide-d_6 99.80 % D (Eurisotop, CAS:2206-27-1), diphenyl ether 99 % (Avocado Research Chemicals Ltd, CAS: 101-84-8), hexyl isocyanate >98.0 % (TCI Europe, CAS: 2525-62-4), JEFFAMINE® T-403 polyetheramine (Huntsman), methanol >99 % (Chem-Lab CAS: 67-56-1), 3-methyl-1-butanol >99.0 % (TCI Europe, CAS: 123-51-3), 2-phenylethanol ≥99 % (Honeywell Fluka™, CAS: 60-12-8), Proton-Sponge® (Sigma-Aldrich, CAS: 20734-58-1), sodium methoxide 25 % wt in methanol (Sigma-Aldrich, CAS: 124-41-4), tetrahydrofuran ≥99.8 % (Fischer Scientific, CAS: 109-99-9), N,N,N′,N′-tetrakis(2-hydroxyethyl)ethylenediamine (Sigma-Aldrich, CAS: 140-07-8) and tributylamine ≥99.0 % (Sigma-Aldrich, CAS: 102-82-9). All reagents and solvents were used as received from their supplier.

2.2 Instrumentation and Characterisation Methods

^{1}H and ^{13}C Nuclear Magnetic Resonance (NMR) spectroscopy. NMR spectra were recorded using a Bruker Avance 300 (300 MHz) or Bruker Ascend 400 (400 MHz). The NMR chemical shifts were reported as δ in parts per million (ppm) relative to the traces of non-deuterated solvent (δ = 7.26 for $CDCl_3$ and δ = 2.50 for DMSO). Data were reported as follows: chemical shift, multiplicity (s = singlet, d = doublet, t = triplet, q '= quadruplet, p = quintuplet, h = hextuplet, hept = heptuplet, m = multiplet, br = broad), coupling constants (*J*) given in Hertz (Hz), and integration values. Standard applied parameters (number of scans, pulse delay, acquisition time, tilt angle, pulse time): ^{1}H spectra (300 MHz: ns = 16, D1 = 1.0 s, AQ = 2.65 s, 30°, P1 = 7.25 µs; 400 MHz: ns = 16, D1 = 1.0 s, AQ = 4.10 s, 30°, P1 = 7.75 µs); ^{13}C spectra (300 MHz: ns = 3072, D1 = 2.0 s, AQ = 1.82 s, 30°, P1 = 7.50 µs; 400 MHz: ns = 3072, D1 = 2.0 s, AQ = 1.36 s, 30°, P1 = 7.50 µs).

Attenuated Total Reflectance - Fourier-Transform Infrared Spectroscopy (ATR-FTIR). ATR-FTIR measurements were performed on a PerkinElmer Spectrum 1000 FTIR spectrometer equipped with Pike ATR module. Spectra were recorded between 4000-600 cm^{-1} with a spectrum resolution of 4 cm^{-1}. All spectra were averaged over 10 scans. Data were reported as follows: wavenumber (cm^{-1}), for defined shapes (br = broad, sh = sharp) and intensity (s = strong, m = medium, w = weak).

Differential Scanning Calorimetry (DSC). DSC measurements were performed on a Mettler Toledo 1/700 calorimeter equipped with a Full Range Sensor (FRS5) sensor containing 56 thermocouples, liquid nitrogen cooling system enabling a temperature range of -150 °C to 700 °C and automatic sample robot. All measurements were carried out under a nitrogen atmosphere in perforated standard 40 µL aluminium crucibles containing 5 – 15 mg of the polymeric material. A consecutive heating-cooling-heating run was performed in a temperature range of -100 °C to 150 °C at a heating/cooling rate of 10 °C min^{-1}. The obtained thermograms were analysed with the STARe Excellence Software and the reported glass transition temperature (T_g) was determined as the midpoint from the second heating run, which is defined as the intercept of the DSC curves and the bisector of the angle formed by the extrapolation of the baselines before and after the transition.

Gas Chromatography–Mass Spectrometry (GC/MS). GC/MS measurements were carried out on an Agilent 6890 GC connected to an Agilent 5973 mass spectrometer, equipped with electrospray ionisation (EI) source and a 2 min splitless injection system. The equipped column was a non-polar Agilent DB-5ms composed of 5% phenyl-dimethyloxane, operated under a 1.3 mL/min constant flow of Helium as a carrier gas at an inlet temperature of 250 °C heated to 320 °C in a heating ramp of 17.5 °C/min after 3 initial min at 70 °C.

High-Resolution Mass Spectrometry (HRMS). High-resolution mass spectrometry (HRMS) has been measured (by direct injection) in a Waters SYNAPTTM G2 HDMSTM, using a Q-TOF detector and (positive) electrospray ionisation ESI+.

Rheology. Rheology experiments were carried out with a Modular Compact Rheometer (MCR) 302 from Anton Paar containing an air-bearing-supported synchronous Electrically Commutated (EC) motor, integrated normal force sensor, TruRate™ sample adaptive controller, TruStrain™ real-time position control and a Convection Temperature Device 180 (CTD 180) heating unit. Measurements were designed and analysed by making use of the RheoCompass™ software. The experiments were performed in parallel plate geometry using 8 mm sample disks, using a normal

force of 1 N, an oscillating frequency of 1 Hz, a strain of 0.8 % and the applied stress was always comprised in the linear viscoelastic region at the measured temperatures. For time sweep experiments, the storage modulus (***G'***) was followed over time at a constant temperature. For stress relaxation experiments, the relaxation modulus (***G'(t)***) was followed over time at a constant temperature. The series of stress relaxation experiments at different temperatures were performed successively on the same sample.

Thermal Gravimetric Analysis (TGA). Thermal gravimetric measurements were performed on a Mettler Toledo TGA/SDTA851e equipped with a Julabo FP50 circulator with HP control unit which is calibrated using three indium pills and approximately 6 mg aluminium. Samples were placed in ceramic pans and heated from 25 °C up to 500 °C at 10 °C min^{-1} under a nitrogen atmosphere. The obtained thermograms were analysed with the STARe Excellence Software and the onset temperature of degradation was defined at 2 % and 5 % weight loss.

Uniaxial tensile tests. Uniaxial tensile testing was performed on a Tinius-Olsen H10KT tensile tester equipped with a 100 N load cell using ASTM standard type IV dog bones (ISO 527-2-2B). The dog bone-shaped samples had an effective gauge length of 12 mm, a width of 2 mm, and a thickness of ±2 mm, and they were cut using a Ray-Ran hand operated cutting press. The tensile measurements were performed using a preload of 0.05 N and a pulling speed of 10 mm min^{-1} until sample failure. The stress σ was recorded as a function of strain ε. Reported values: elongation (%), stress at break (Pa), and Young's modulus (Pa) are the average and standard deviations of at least seven samples. Exhibited tensile curves were selected to be representative of the average values.

2.3 Experimental procedures

Model Compound Studies. Three model study tests were performed to assess the exchange reactions in the presence of an excess of alcohol groups (Fig. 2.A-C). The experiments were performed by mixing the chosen model compounds (0.90 mmol, 1 eq.) with 2-phenylethanol (4.50 mmol, 5 eq.) and stirring for 72 h at 130 °C in a sealed vial. Then, all reaction mixtures were analysed through ^{1}H-NMR and GC-MS and compared with the initial batches. Two additional model study tests were carried out to evaluate the carbamate exchange reactions in the absence of alcohols (Fig. 3.A,D). The experiments were performed under the same conditions used in the previous tests with a mixture of two of the selected model compounds (2.30 mmol, 1 eq.). For subsequential analyses, the mixtures were subjected to GC-MS and FT-IR.

Network Processing and Reprocessability Tests. Samples were processed by compression moulding at 130 °C for 30 min under 1.5 – 2 Mt in a steel mould. In order to release the applied load gradually during the decompression step, the heating system was disconnected at a slow overnight decompression rate and cooling effect in a steel rectangular mould (A: 70 mm x 40 mm x 2 mm; B: 30 mm x 15 mm x 2 mm). Reprocessability tests, performed complementarily to the uniaxial tensile measurements, consisted in cutting and compressing small fragments from broken dog bones and the excess of material from the previous processing cycle. The resulting samples were then folded in half and pressed again to give a fully healed material.

Network Solubility Tests. Solubility tests were carried out using two pairs of discs of 6 mm diameter and 2 mm thickness, cut from networks that were processed one time and reprocessed five times. The samples were immersed in 5 mL of diphenyl ether,[45] placed in sealed vials kept at room

temperature and 100 °C for 24 h respectively (Fig. S9). The discs were then dried under vacuum overnight at 65 °C. The swelling ratios and soluble fractions were calculated using equations (1) and (2), respectively, where m_0, m_s, m_d are the initial, swollen and dry masses of the respective samples.

$$Swelling\ Ratio\ (\%) = \frac{m_s - m_0}{m_0} \quad (1)$$

$$Soluble\ Fraction\ (\%) = \frac{m_0 - m_d}{m_0} \quad (2)$$

Additionally, solubility experiments were performed at 25 °C and 130 °C using diethylethanolamine and 2-phenylethanol to evaluate the effect of different hydroxylated solvents and temperatures. This test was conceived to evaluate if the material would undergo exchange reactions without any applied mechanical stress. (Fig. S10).

3 Results and Discussion

3.1 Model Studies

Both dissociative and associative exchange mechanisms have been previously reported to take place in polyhydroxyurethane-based dynamic materials.[21] Associative transcarbamoylation reactions mainly compete with reverse urethane dissociation and reverse cyclic carbonate formation. In order to investigate whether the tertiary amine groups also have a proximity-induced internal catalytic effect[30] when introduced at the oxygen side of the carbamate (but keeping the bond distance to the carbonyl unit unaltered), nine low molecular weight compounds [**MC1 to MC9,** (Table S1)] with an **R_3N_β-O** motif were synthesized and subjected to transcarbamoylation model studies (Figs. 2,3). In a first transcarbamoylation test reaction (reaction **A**, Fig. 2.A), model carbamate **MC1** was heated at 130 °C in the presence of 5 equivalents 2-phenylethanol to assess the exchange dynamics in the absence of a tertiary amine catalyst. Analysis of the obtained reaction mixture through gas chromatography – mass spectrometry (GC-MS) (Fig. 2.C) indicated that no exchange product **MC2** formed after 72 hours at 130 °C. Repeating the model reaction in the presence of one equivalent of tributylamine, acting as an external catalyst, also yielded no exchange product being detected through GC-MS and ^{1}H-NMR (Fig. 2.A and Fig. S5). In contrast, reaction **B** with model compound **MC3** (containing the **R_3N_β-O**), (Fig. 2.B), did yield the expected exchange product since **MC2** could be detected *via* GC-MS analysis (Fig. 2.D). The exchange conversion of this last reaction was calculated using ^{1}H-NMR by comparing the integrals of the signals of the methylenes in alfa-position of the oxygen of the carbamate bonds of **MC2** with their counterpart in **MC3**. This method gave a conversion of about 58%. However, this could be only interpreted as an approximation due to the presence of small overlapping impurities (Fig. S6). A second approximation of this value was obtained based on the decrease of the integration of the relative area of the starting compounds observed by GC (Fig. 2D), which gave a similar value of 60 %.

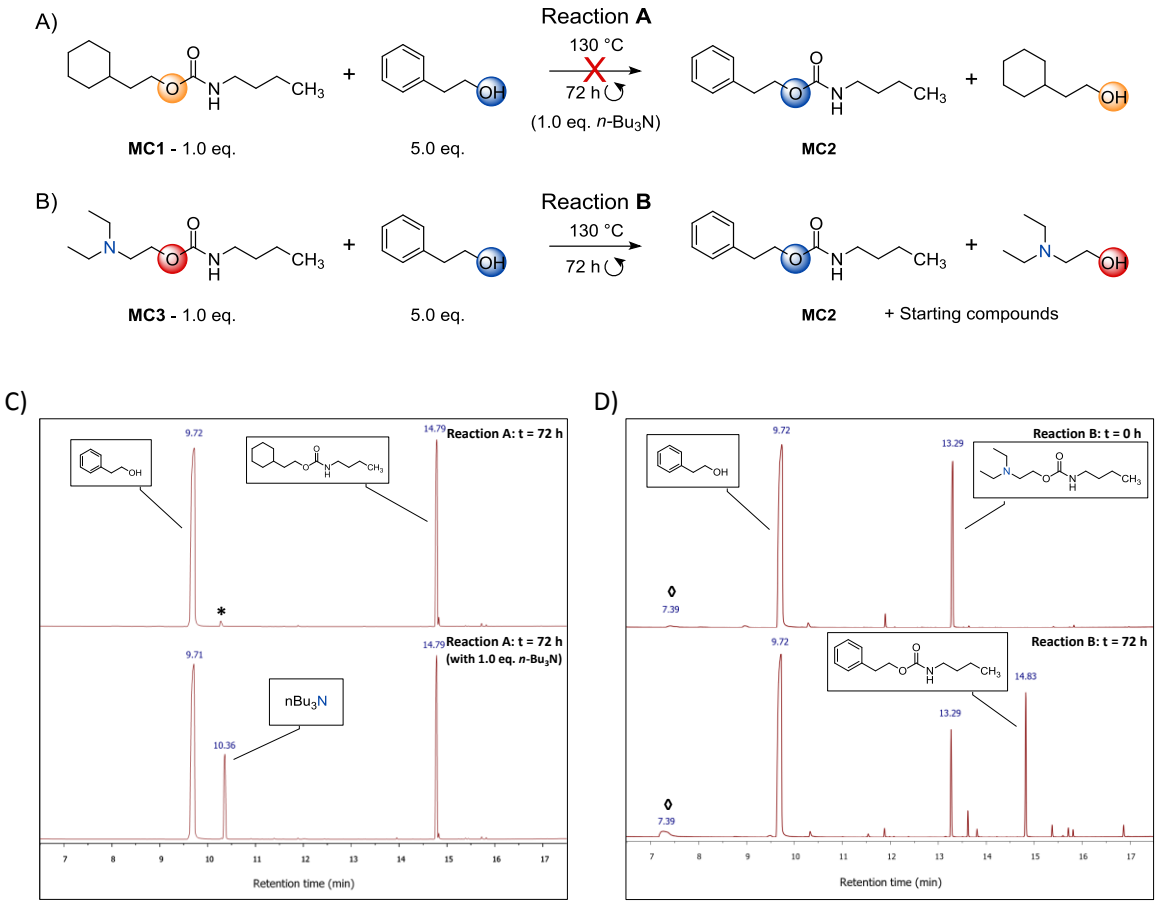

Fig. 2. Overview of transcarbamoylation model studies. **A**) Exchange reaction A of tertiary amine-free **MC1** with an excess of 2-phenylethanol (5 eq.) both in the absence and presence of nBu$_3$N (1 eq.) as an external catalyst (no exchange product detected). **B**) Internally catalysed exchange reaction of **MC3** with 2-phenylethanol (5 eq.) resulting in the formation of exchange product **MC2**. **C)** GC chromatogram of the crude resulting from reaction **A** without (after 72 h, top) and with external catalyst (after 72 h, bottom). **D)** GC chromatogram of the crude resulting from reaction **B** before (t = 0 h, top) and after heating (t = 72 h, bottom). ***Note that the trace signal detected at 10.26 min does not correspond to the tributylamine signal, but to a small amount of a degradation product barely visible in the chromatogram below. $^{\lozenge}$The explanation for the presence of alcohol and isocyanate signals on the GC-MS chromatograms can be found in the SI.

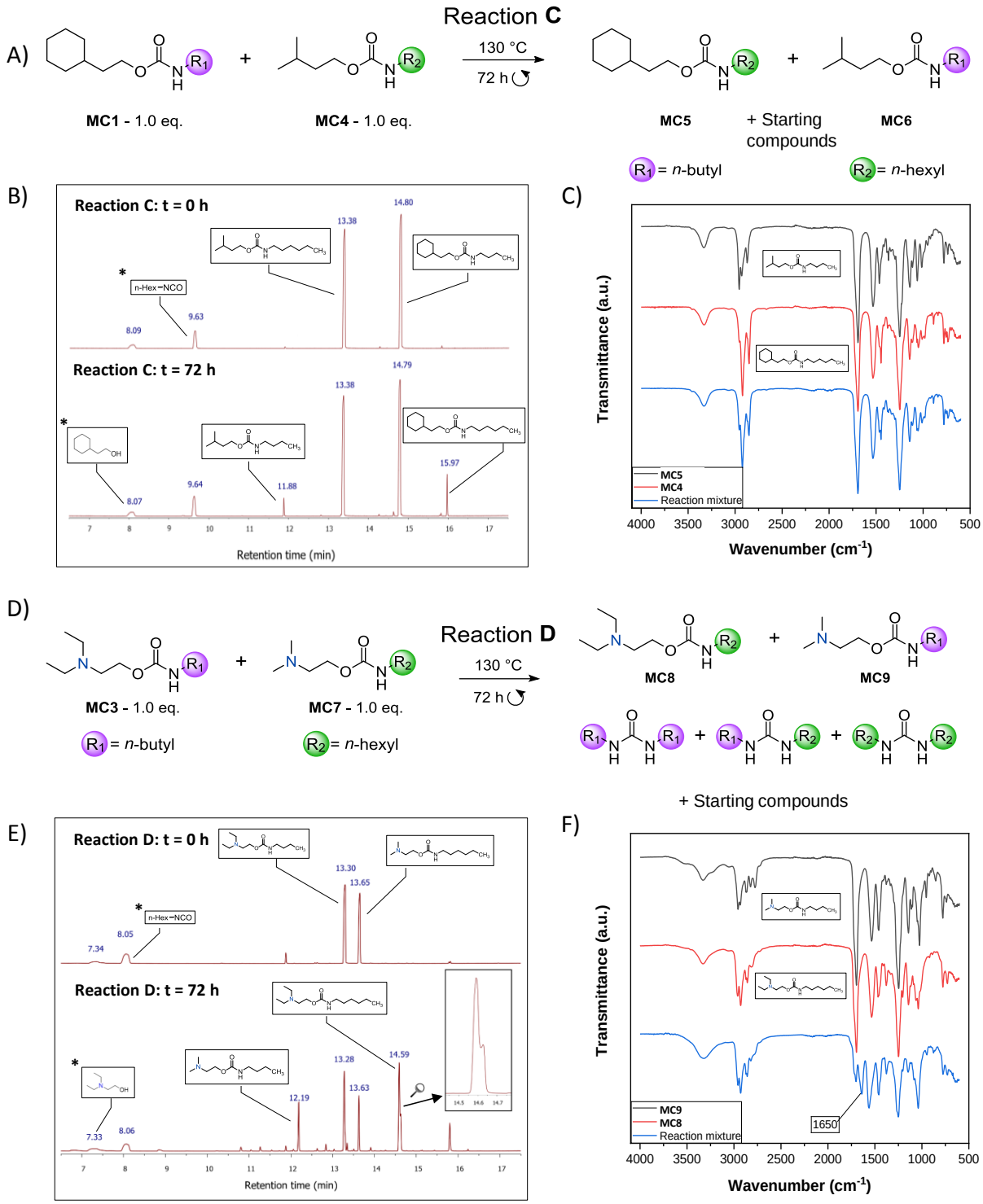

Fig. 3. A) N-catalysed carbamate exchange model reaction between **MC1** and **MC4** to form **MC5** and **MC6**. **B)** GC chromatograms from reaction mixture **C** at t = 0 h (top) and t = 72 h (bottom). **C)** ATR-FTIR spectra of isopentyl butylcarbamate **MC6** (black), 2-cyclohexylethyl hexylcarbamate **MC6** (red) and reaction mixture **C** at t = 72 h (blue). **D)** Internally catalysed carbamate exchange model reaction between **MC3** and **MC7** to form **MC8** and **MC9**, along with additional urea products. **E)** GC chromatograms from the reaction mixture **D** at t = 0 h (top) and t = 72 h (bottom). **F)** ATR-FTIR spectra of 2-(dimethylamino)ethyl butylcarbamate **MC9** (black), 2-(diethylamino)ethyl hexylcarbamate **MC8** (red) and reaction mixture **D** at t = 72 h (blue). *The explanation for the presence of alcohols and isocyanates on the GCMS chromatograms is detailed in the SI.

A second range of model experiments was conducted utilizing only a mixture of two different carbamates to examine whether carbamate exchange can proceed also in the absence of alcohols (reaction **C** (Fig. 3.A). Heating an equimolar mixture of the amine-free carbamates **MC1** and **MC4**, exchange products peaks were observed by GC-MS (Fig. 3.B) (**MC5** and **MC6)**, despite the absence of tertiary amines or hydroxyl groups in the system. Nonetheless, in the results observed for reaction **D** (Fig. 3.D), in which an equimolar mixture of **R_3N_β-O** carbamates was used, the CG chromatogram (Fig. 3.E) showed more relatively intense exchange product peaks (**MC8** and **MC9)** when compared to the signals of the remaining **MC3** and **MC7** and even when compared to the alcohol and isocyanate signals formed during the GC-MS analyses. It should be noted that reactions C and D could only be analysed qualitatively since their conversions could not be followed through ^{1}H-NMR due to the signal similarity between the original and the exchange products. Because of this, the obtention of the reaction yields though GC relative peak area integrations could not be cross checked and verified.

It should be noted that the presence of tertiary amines also resulted in additional side reactions. This was evidenced by the higher amount of undetermined side products that could be detected in the gas chromatogram of the crude mixture of reaction **D** (Fig. 3.D) compared to reaction **C** (Fig. 3.A). Furthermore, FT-IR analyses confirmed the formation of urea products with their characteristic C=O stretching signal at 1650 cm^{-1} in the outcome of reaction **D** (Fig. 3.F). Presence of ureas was further confirmed by High Resolution Mass Spectrometry (HRMS) analyses of the obtained product mixture from reaction **D**, in which of *N*,*N'*-dibutylurea and *N*,*N'*-dihexylurea were detected (Fig. S7). Considering the absence of the unequivocal isocyanate stretching signal usually found between 2270 – 2240 cm^{-1} in all FT-IR analyses performed (Figs. 3.C,F), it could not be concluded if the carbamate exchanges occurred as a result of a urethane dissociation mechanism with the formation of isocyanates and alcohols.

Some authors have suggested that PHU-based networks are able to dissociate to cyclic carbonates and amine groups, under specific conditions.[21] Moreover, in the presence of strong bases such as 1,5,7-triazabicyclo(4.4.0)dec-5-ene (TBD), it has been shown that the newly formed amines are able to react with carbamate groups to form linear ureas.[39] Then, thermally-induced urea exchange reactions would start to take place between ureas and free amines.[53] Yet, the reaction between tertiary amine-free carbamates indicates the possibility of an exchange mechanism where isocyanates are not involved, since the absence of the formation of **MC1** in reaction **A** (Fig. 2.A) and the absence of isocyanates in the FT-IR spectra (Fig. 3.C) lead to the conclusion that no isocyanates got released during model reaction **A** (with and without one equivalent of tributylamine). Based on these results, we could conclude that there is evidence for an internal basic or nucleophilic catalytic effect of beta tertiary amines on associative/dissociative mechanisms involving carbamate linkages, similar to the ones observed in the presence of strong bases. In (Fig. 4), two possible reaction schemes are proposed on how an internal catalyst could trigger the exchange reaction known for polyhydroxyurethanes[21] as well as the linear urea formation in **IC-NIPU** networks, i.e. thorugh associative transcarbamoylation (Fig. 4.A) (also applicable to **R_3N_β-N** carbamates), and urethane dissociation followed by base catalysed linear urea formation (Fig. 4.B) (only applicable to **R_3N_β-O** carbamates).

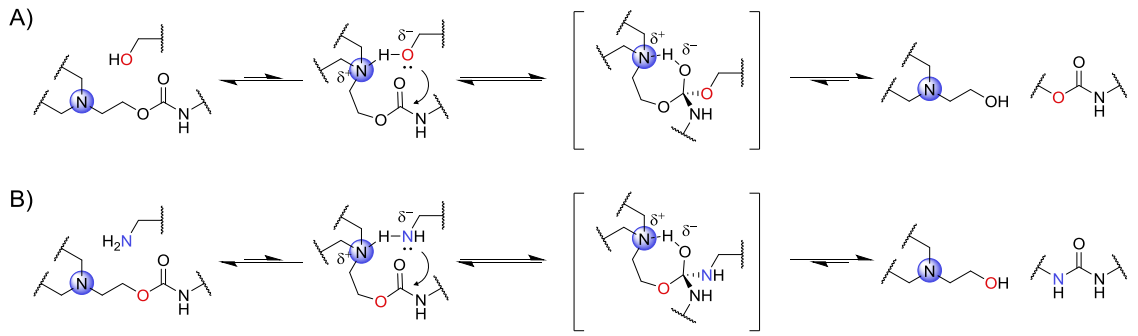

Fig. 4. Proposed reaction mechanisms of the basic internal catalysis for the **A**) associative transcarbamoylation and **B**) base catalysed linear urea formation.[39]

3.2 Synthesis of R_3N_β-O-based Network

As the beta-amino groups along the carbamate-oxygen side proved to promote exchange product formation, the following step in our investigation was the preparation of a covalently crosslinked material containing the embedded **R_3N_β-O** groups. Thus, an **IC-NIPU** was synthesized from the dicyclic 8-membered ring carbonate monomer (**BN8C**), previously reported by Sardon and co-workers,[54] and JEFFAMINE® T-403 as a multifunctional amine crosslinker (Fig. 5). In order to obtain 6.00 g of the BN8C-JAT403-Network (Fig. 5), BN8C (3.00 g, 10.32 mmol, 3.00 eq.) and JEFFAMINE® T-403 Polyetheramine (3.12 mL, 6.84 mmol, 2.00 eq.) were mixed in a 60 mL polypropylene cup. To disperse the solid **BN8C** into the viscous amine crosslinker to obtain a homogeneous dispersion a DAC 150.1 FVZ speed mixer was used at 2500 rpm for 2 min. Then, the mixed sample was kept 24 h at room temperature. The curing process was performed without any solvent or external catalyst by keeping the neat samples at 100 °C for 3 h. The result was an opaque white soft elastomer polyhydroxyurethane (Fig. 8. A1), which turned to a transparent yellow and more amber in colour material upon reprocessing by hot pressing (Fig. 8A). The material was subsequently characterized through Fourier-Transform Infrared Spectroscopy (FT-IR), solubility tests, Thermogravimetric Analysis (TGA), Differential Scanning Calorimetry (DSC) and uniaxial tensile tests in order to determine the structure and thermomechanical properties of the targeted network.

The obtained FT-IR spectrum of the as synthesized **IC-NIPU** network showed the characteristic signals of the polyether prepolymer segments and was shown to contain polyhydroxyurethanes, identified by the broad O-H stretches of the hydroxyl groups around 3400 cm^{-1} and H-bonded carbamate C=O stretching bands at 1726 cm^{-1} (Fig. 8.B). Calculated gel fractions of a one-time processed network obtained through swelling tests in diphenyl ether[45] at 25 °C and 100 °C were 99.6 % and 89.4 %, respectively (Table S4). When using an excess of 2-diethylethanolamine and 2-phenylethanol as reactive solvents, full solubility of the crosslinked materials was obtained at 130 °C, proving that they undergo dynamic exchange reactions without any applied mechanical stress at elevated temperatures (Fig. S10). TGA analyses showed the degradation temperatures corresponding to a 2 % and 5 % weight loss to be 148 °C and 175 °C, respectively (Fig. S12). Additionally, glass transition temperatures (T_g) derived from the second heating run of DSC experiments on samples processed from one to four times were detected within the temperature interval of -20 °C to -16 °C (Fig. S13), as can be expected for a soft rubbery material with slight crosslink density fluctuations originated from the contribution of a dissociative bond exchange process. One-time processed samples had an average Young's modulus of 0.45 ± 0.02 MPa, a total elongation of 132 ± 21 %, and

ultimate stress of 0.40 ± 0.05 MPa in uniaxial tensile tests (Table 1). Overall, the obtained FT-IR, TGA, solubility and reprocessing results are within those expected for a crosslinked dynamic elastomeric material.

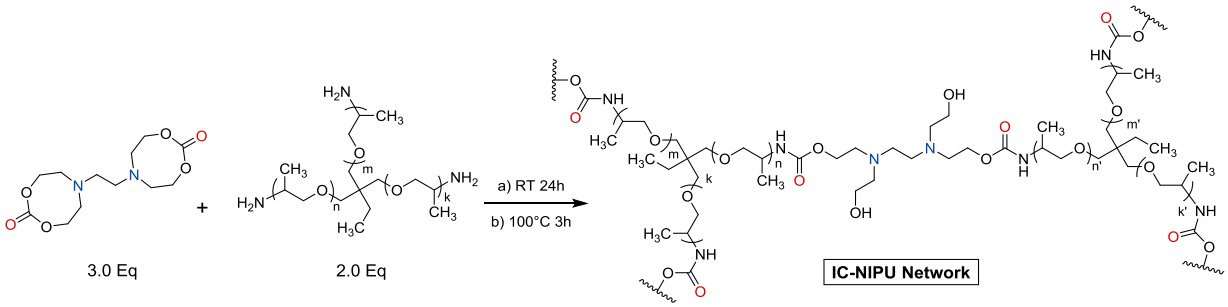

Fig. 5. Reaction scheme for the synthesis of **IC-NIPU** materials.

3.3 Rheological analysis

Following the insights into the internal catalytic effect of the tertiary amine on the small molecule transcarbamoylation reaction, a material level study was conducted to evaluate the dynamic bond exchange properties within the synthesized R_3N_β-O-based **IC-NIPU** network. Viscoelastic properties can be studied through stress-relaxation experiments upon applying a constant deformation at a certain temperature. The relaxation times (***τ****) were calculated in a defined temperature interval when (***G/G₀***) equalled to 1/e, where (***G***) is the relaxation modulus, (***G₀***) the relaxation modulus at t = 0.[14,15] The obtained results from the measurements performed by subjecting the material to 0.8 % deformation from high (i.e. 150 °C) to low temperatures confirmed the dynamic behaviour of the **R_3N_β-O IC-NIPU** network with a decrease of the relaxation modulus G(t) over time. Relaxation times (**τ***) were determined as the measurement time at which **G/G_0** equals 1/e throughout a temperature interval of 150 – 100 °C (Fig. 6.A).

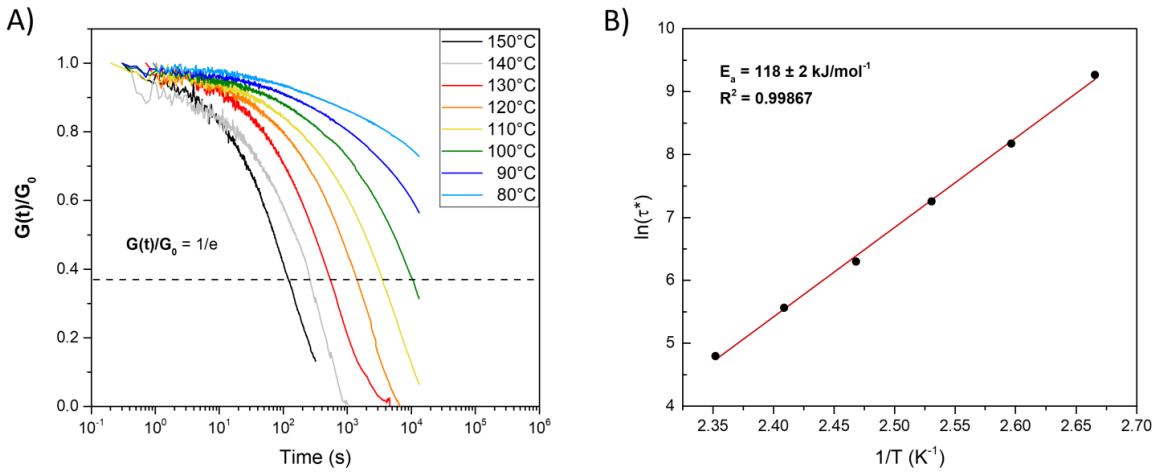

Fig. 6. A) IC-NIPU network stress-relaxation curves obtained at different temperatures ranging from 150 °C down to 80 °C. **B)** Arrhenius plot of **R_3N_β-O IC-NIPU** relaxation times between 100 °C and 150 °C with a linear correlation.

The studied network seemed to fit a single Maxwell decay model, as the system displayed a linear correlation of relaxation times within the described temperature range (Fig. 6.B). This result could indicate a pure associative nature or that the expected dissociative mechanisms still allowed for the material to maintain efficiently crosslinked states at the studied temperature interval. Additionally, the observed activation energy ($\boldsymbol{E_a}$ = 118 ± 2 kJmol^{-1}) had a similar value in comparison to the catalyst-free polyhydroxyurethane- vitrimers reported by Hillmyer and co-workers[21,45], which included a $\mathbf{R_3N_\beta}$**-N** amines at the same distance yet opposite side to the carbonyl groups as the network studied herein. Both results seem to indicate that the internal catalytic effect of tertiary amines on the transcarbamoylation rather relies on the proximity between the tertiary amino group and the carbonyl of the urethane group, rather than on the position in relation to the carbamate functionality.

Although the here synthesized **IC-NIPU** network displays stress relaxation properties that are consistent to structurally related CAN materials, the relaxation modulus at t = 0 ($\boldsymbol{G_0}$) showed a significant drop after the first stress relaxation measurement at 150 °C and its value increased as the temperature was lowered before each successive measurement (Fig. 7.A). This observation hinted toward a dissociative contribution that was not detected during the initial measurement, most likely because the material was only briefly exposed to high temperatures. To further investigate this phenomenon, the storage modulus values were obtained *via* time sweep experiments at different temperatures starting from 150 °C down to 100 °C (Fig. 7.B) following an initial annealing step at 150 °C for 10 minutes to allow for the system to equilibrate. According to Flory's molecular theory of elasticity,[2,55] a partial reduction of the crosslink density in a polymeric network is described to result in a reduction of the storage modulus of the material. This can be easily understood through a reformulation of Flory's equation made by Kloxin and Bowman,[6] which describes a linear effect of the crosslink density on the elastic modulus of a material through equation (3) where only the storage modulus (***E***), crosslink density ($\boldsymbol{\rho_x}$), temperature (***T***) and the universal gas constant (***R***) have to be considered. As expected, the storage moduli obtained from the time sweep experiments (Fig. 7.B) thus indicated that the network was less densely crosslinked during the first stress relaxation measurement at 150 °C. As the temperature was lowered for every consecutive measurement, the system experienced progressive crosslink density recovery with increasing storage modulus as a result of the re-establishment of the dissociative exchange equilibrium, favouring an increasing extent of bond connectivity until the temperature was low enough to suppress the dissociative exchange.

$$E = \rho_x RT \qquad (T \gg T_g) \qquad (3)$$

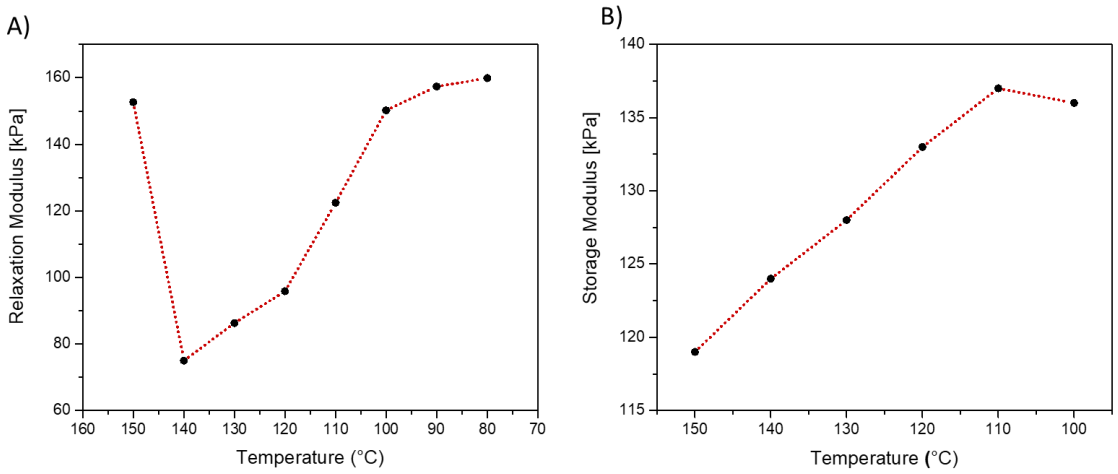

Fig. 7. A) Relaxation modulus values at t = 0 at temperatures ranging from 150 °C to 80 °C. **B)** Average storage modulus values at the temperatures at which the material's relaxation times could be determined (Fig. 6.A).

3.4 Network Recyclability

Finally, the mechanical properties of reprocessed **IC-NIPU** networks were studied to evaluate the recyclability potential of the material by compression moulding at 130 °C for 30 min under 1.5 – 2 Mt in a steel mould. In order to release the applied load gradually during the decompression step, the hot press was switched off at a slow overnight decompression and cooling rate to allow for the dissociative bond exchange mechanism to regenerate the lost crosslinking density. Next, dog bones cut from a sample processed once and five consecutive times at 130 °C were subjected to uniaxial tensile measurements (Fig. 8.C). The stress (***σ***) was recorded as a function of strain (***ε***) and the obtained elongation (***%***), ultimate stress, and Young's modulus are given as the average of seven samples (Table 1). The measurements revealed a decrease in the Young's modulus, most likely attributed to degradation of the samples, which also turned the material more amber in colour after each cycle (Fig. 8.A). The occurrence of side reactions was confirmed by ATR-FTIR of the reprocessed network, with urea C=O stretching formation detected at 1650 cm^{-1} that became more intense after each reprocessing cycle (Fig. 8.B). These side reactions were able to turn the IC-NIPU into a poly(hydroxyurea–urethane) network, which has been shown in previous research to lead to a significant enhancement in the phase separation behaviour of NIPUs.[53] Additionally, in order to further establish the effect of temperature on the urea formation, an additional recycling test was performed at 160 °C to test the effect of higher temperatures on degradation and faster urea formation upon reprocessing. For this, a freshly synthesized network was recycled four times by compression moulding at 160 °C using the same conditions as detailed above (i.e. 30 minutes) with a significantly more rapid degradation and urea formation being detected, since the material turned brown already after the first processing. During the following cycles, coloration became more pronounced and the network showed a progressive loss of its dimensional stability, resulting in a viscous paste after the 4^{th} reprocessing (Fig. S14.1). ATR-FTIR analyses taken after each cycle confirmed the faster urea signal intensity increase (Fig. S14.2). Nonetheless, the data obtained from the tensile tests confirmed that the synthesized material can be successfully reprocessed at 130 °C while partially retaining its mechanical properties and keeping its thermal behaviour, with only slight changes detected in the network's T_g that remained within the interval comprised between -20 °C and -16 °C (Fig. S13).

Table 1. Ultimate stress, elongation and Young's modulus derived from uniaxial tensile tests performed on the (re)processed **IC-NIPU** samples.

(Re)Processing Cycle	Ultimate Stress (MPa)	Total Elongation (%)	Young's Modulus (MPa)
1st	0.40 ± 0.05	132 ± 21	0.45 ± 0.02
5th	0.28 ± 0.03	135 ± 17	0.41 ± 0.07

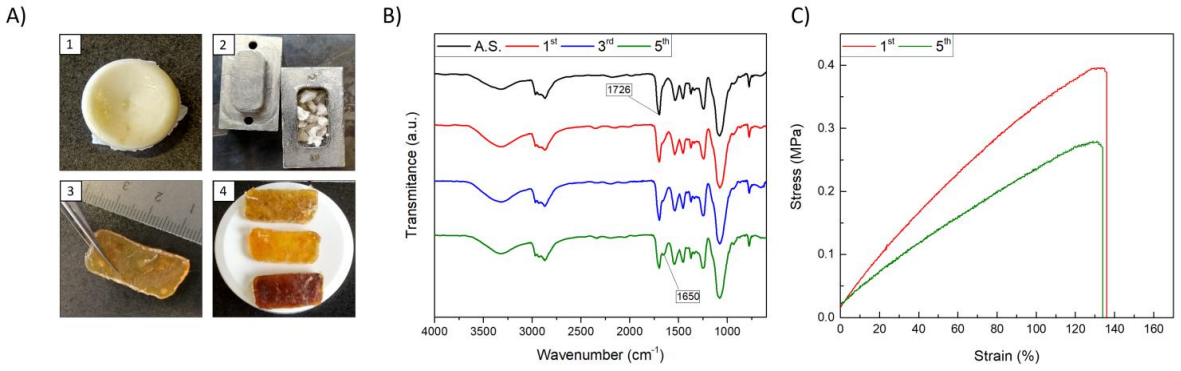

Fig. 8. A) Pictures of the **IC-NIPU** samples (1) As synthesized, (2) shredded and prepared for compression-moulding, (3) after one-time processing (130 °C for 30 min under 1.5 – 2 Mt), (4) after (top to bottom) one, three and five-times (re)processing. **B)** ATR-FTIR spectra of as synthesized (A.S., black), one (red), three (blue) and five (green) times (re)processed **IC-NIPU** network at 130°C. **C)** Representative uniaxial tensile stress measurements of **IC-NIPU** samples after a **1st** (red) and **5th** (green) (re)processing step.

4 Conclusions

In this work, we demonstrated the importance of internal catalysis in the dynamic behaviour of non-isocyanate polyurethanes based on N-substituted 8-membered cyclic carbonates and macromolecular amines. The exchange reactions between carbamates were qualitatively proven to be more effective on internally catalysed samples, although urea formation was also detected. Due to the formation of these urea groups, the **IC-NIPU** material experienced a crosslink density decrease upon reprocessing as shown by stress relaxation experiments.[21] Nonetheless, the materials maintained a sufficiently crosslinked state during the measurements to fit a single Maxwell decay Arrhenian model, likely attributed to the contribution of an associative transcarbamoylation exchange mechanism. In spite of the similarity of the observed activation energy of the herein synthesized **R_3N_β-O**-based **IC-NIPU** network with the system reported by Hillmyer and co-workers[45], the presence of urea groups indicates a more complicated dynamic exchange pathway. While the internal catalytic effect of the tertiary amine within the system seems to rely only on the proximity between the amino group and the carbonyl moieties, rather than on the location of the amino group, the presence of the **R_3N_β-O** functionality proved to catalyse side reactions that involve urea formation. In general, this study emphasized the role and helped for the understanding of internal catalysis in the research area of CANs. Particularly in polyurethane-based systems, the ability to control urea formation without significantly affecting the crosslinking density stands as an appealing feature to be further investigated to enhance the potential of these internally catalysed non-isocyanate CANs [53].

Declaration of Competing Interest

The authors declare that they have no known competing financial interests or personal relationships that could have appeared to influence the work reported in this paper.

Acknowledgements

This project has received funding from the European Union's Horizon 2020 research and innovation programme under the Marie Skłodowska-Curie Grant agreement No 860911. The authors thank Bernhard De Meyer and Jan Goeman for technical support and Dr. Yann Spiesschaert and Filip van Lijsebetten for their fruitful discussions.

Disclaimer

This article reflects only the authors' view. The European Union is not liable for any use that may be made of the information contained herein.

Appendix A. Supplementary material

Supplementary data to this article can be found online at (**to be provided**)

The raw data required to reproduce these findings are available upon request to the corresponding author. The processed data required to reproduce these findings are available upon request to the corresponding author.

References

[1] A. Shenoy, D. Saini, Thermoplastic Melt Rheology and Processing, 1996.

[2] P.J. Flory, Network Structure and the Elastic Properties of Vulcanized Rubber., Chem. Rev. 35 (1944) 51–75. https://doi.org/10.1021/cr60110a002.

[3] M. Toozandehjani, Conventional and Advanced Composites in Aerospace Industry: Technologies Revisited, AJAE. 5 (2018) 9. https://doi.org/10.11648/j.ajae.20180501.12.

[4] C.J. Kloxin, T.F. Scott, B.J. Adzima, C.N. Bowman, Covalent Adaptable Networks (CANs): A Unique Paradigm in Cross-Linked Polymers, Macromolecules. 43 (2010) 2643–2653. https://doi.org/10.1021/ma902596s.

[5] C.N. Bowman, C.J. Kloxin, Covalent Adaptable Networks: Reversible Bond Structures Incorporated in Polymer Networks, Angew. Chem. Int. Ed. 51 (2012) 4272–4274. https://doi.org/10.1002/anie.201200708.

[6] C.J. Kloxin, C.N. Bowman, Covalent adaptable networks: smart, reconfigurable and responsive network systems, Chem. Soc. Rev. 42 (2013) 7161–7173. https://doi.org/10.1039/C3CS60046G.

[7] P. Cordier, F. Tournilhac, C. Soulié-Ziakovic, L. Leibler, Self-healing and thermoreversible rubber from supramolecular assembly, Nature. 451 (2008) 977–980. https://doi.org/10.1038/nature06669.

[8] J. Fox, J.J. Wie, B.W. Greenland, S. Burattini, W. Hayes, H.M. Colquhoun, M.E. Mackay, S.J. Rowan, High-Strength, Healable, Supramolecular Polymer Nanocomposites, J. Am. Chem. Soc. 134 (2012) 5362–5368. https://doi.org/10.1021/ja300050x.

[9] A. Bossion, I. Olazabal, R.H. Aguirresarobe, S. Marina, J. Martín, L. Irusta, D. Taton, H. Sardon, Synthesis of self-healable waterborne isocyanate-free poly(hydroxyurethane)-based supramolecular networks by ionic interactions, Polym. Chem. 10 (2019) 2723–2733. https://doi.org/10.1039/C9PY00439D.

[10] H.A. Houck, E. Blasco, F.E. Du Prez, C. Barner-Kowollik, Light-Stabilized Dynamic Materials, J. Am. Chem. Soc. 141 (2019) 12329–12337. https://doi.org/10.1021/jacs.9b05092.

[11] F. García, J. Pelss, H. Zuilhof, M.M.J. Smulders, Multi-responsive coordination polymers utilising metal-stabilised, dynamic covalent imine bonds, Chem. Commun. 52 (2016) 9059–9062. https://doi.org/10.1039/C6CC00500D.

[12] A. Gandini, The furan/maleimide Diels–Alder reaction: A versatile click–unclick tool in macromolecular synthesis, Progress in Polymer Science. 38 (2013) 1–29. https://doi.org/10.1016/j.progpolymsci.2012.04.002.

[13] J.M. Winne, L. Leibler, F.E. Du Prez, Dynamic covalent chemistry in polymer networks: a mechanistic perspective, Polym. Chem. 10 (2019) 6091–6108. https://doi.org/10.1039/C9PY01260E.

[14] D. Montarnal, M. Capelot, F. Tournilhac, L. Leibler, Silica-Like Malleable Materials from Permanent Organic Networks, Science. 334 (2011) 965–968. https://doi.org/10.1126/science.1212648.

[15] M. Capelot, D. Montarnal, F. Tournilhac, L. Leibler, Metal-Catalyzed Transesterification for Healing and Assembling of Thermosets, J. Am. Chem. Soc. 134 (2012) 7664–7667. https://doi.org/10.1021/ja302894k.

[16] W. Denissen, J.M. Winne, F.E. Du Prez, Vitrimers: permanent organic networks with glass-like fluidity, Chem. Sci. 7 (2016) 30–38. https://doi.org/10.1039/C5SC02223A.

[17] A. Jourdain, R. Asbai, O. Anaya, M.M. Chehimi, E. Drockenmuller, D. Montarnal, Rheological Properties of Covalent Adaptable Networks with 1,2,3-Triazolium Cross-Links: The Missing Link between Vitrimers and Dissociative Networks, Macromolecules. 53 (2020) 1884–1900. https://doi.org/10.1021/acs.macromol.9b02204.

[18] G.M. Scheutz, J.J. Lessard, M.B. Sims, B.S. Sumerlin, Adaptable Crosslinks in Polymeric Materials: Resolving the Intersection of Thermoplastics and Thermosets, J. Am. Chem. Soc. 141 (2019) 16181–16196. https://doi.org/10.1021/jacs.9b07922.

[19] J. Shi, T. Zheng, Y. Zhang, B. Guo, J. Xu, Cross-linked polyurethane with dynamic phenol-carbamate bonds: properties affected by the chemical structure of isocyanate, Polym. Chem. 12 (2021) 2421–2432. https://doi.org/10.1039/D1PY00157D.

[20] B.R. Elling, W.R. Dichtel, Reprocessable Cross-Linked Polymer Networks: Are Associative Exchange Mechanisms Desirable?, ACS Cent. Sci. 6 (2020) 1488–1496. https://doi.org/10.1021/acscentsci.0c00567.

[21] D.J. Fortman, J.P. Brutman, M.A. Hillmyer, W.R. Dichtel, Structural effects on the reprocessability and stress relaxation of crosslinked polyhydroxyurethanes: ARTICLE, J. Appl. Polym. Sci. 134 (2017) 44984. https://doi.org/10.1002/app.44984.

[22] J.L. Self, N.D. Dolinski, M.S. Zayas, J. Read de Alaniz, C.M. Bates, Brønsted-Acid-Catalyzed Exchange in Polyester Dynamic Covalent Networks, ACS Macro Lett. 7 (2018) 817–821. https://doi.org/10.1021/acsmacrolett.8b00370.

[23] F. Elizalde, R.H. Aguirresarobe, A. Gonzalez, H. Sardon, Dynamic polyurethane thermosets: tuning associative/dissociative behavior by catalyst selection, Polym. Chem. 11 (2020) 5386–5396. https://doi.org/10.1039/D0PY00842G.

[24] P. Yan, W. Zhao, X. Fu, Z. Liu, W. Kong, C. Zhou, J. Lei, Multifunctional polyurethane-vitrimers completely based on transcarbamoylation of carbamates:

thermally-induced dual-shape memory effect and self-welding, RSC Adv. 7 (2017) 26858–26866. https://doi.org/10.1039/C7RA01711A.

[25] D.J. Fortman, D.T. Sheppard, W.R. Dichtel, Reprocessing Cross-Linked Polyurethanes by Catalyzing Carbamate Exchange, Macromolecules. 52 (2019) 6330–6335. https://doi.org/10.1021/acs.macromol.9b01134.

[26] W. Denissen, G. Rivero, R. Nicolaÿ, L. Leibler, J.M. Winne, F.E. Du Prez, Vinylogous Urethane Vitrimers, Adv. Funct. Mater. 25 (2015) 2451–2457. https://doi.org/10.1002/adfm.201404553.

[27] N. Zheng, J. Hou, Y. Xu, Z. Fang, W. Zou, Q. Zhao, T. Xie, Catalyst-Free Thermoset Polyurethane with Permanent Shape Reconfigurability and Highly Tunable Triple-Shape Memory Performance, ACS Macro Lett. 6 (2017) 326–330. https://doi.org/10.1021/acsmacrolett.7b00037.

[28] S. Debnath, S. Kaushal, U. Ojha, Catalyst-Free Partially Bio-Based Polyester Vitrimers, ACS Appl. Polym. Mater. 2 (2020) 1006–1013. https://doi.org/10.1021/acsapm.0c00016.

[29] R. Sustmann, A simple model for substituent effects in cycloaddition reactions. II. The diels-alder reaction, Tetrahedron Letters. 12 (1971) 2721–2724. https://doi.org/10.1016/S0040-4039(01)96962-X.

[30] F. Van Lijsebetten, J.O. Holloway, J.M. Winne, F.E. Du Prez, Internal catalysis for dynamic covalent chemistry applications and polymer science, Chem. Soc. Rev. 49 (2020) 8425–8438. https://doi.org/10.1039/D0CS00452A.

[31] O.R. Cromwell, J. Chung, Z. Guan, Malleable and Self-Healing Covalent Polymer Networks through Tunable Dynamic Boronic Ester Bonds, J. Am. Chem. Soc. 137 (2015) 6492–6495. https://doi.org/10.1021/jacs.5b03551.

[32] C. Hao, T. Liu, S. Zhang, W. Liu, Y. Shan, J. Zhang, Triethanolamine-Mediated Covalent Adaptable Epoxy Network: Excellent Mechanical Properties, Fast Repairing, and Easy Recycling, Macromolecules. 53 (2020) 3110–3118. https://doi.org/10.1021/acs.macromol.9b02243.

[33] M. Delahaye, J.M. Winne, F.E. Du Prez, Internal Catalysis in Covalent Adaptable Networks: Phthalate Monoester Transesterification As a Versatile Dynamic Cross-Linking Chemistry, J. Am. Chem. Soc. 141 (2019) 15277–15287. https://doi.org/10.1021/jacs.9b07269.

[34] C. Taplan, M. Guerre, F.E. Du Prez, Covalent Adaptable Networks Using β-Amino Esters as Thermally Reversible Building Blocks, J. Am. Chem. Soc. 143 (2021) 9140–9150. https://doi.org/10.1021/jacs.1c03316.

[35] H. Zhang, S. Majumdar, R.A.T.M. van Benthem, R.P. Sijbesma, J.P.A. Heuts, Intramolecularly Catalyzed Dynamic Polyester Networks Using Neighboring Carboxylic and Sulfonic Acid Groups, ACS Macro Lett. 9 (2020) 272–277. https://doi.org/10.1021/acsmacrolett.9b01023.

[36] M. Podgórski, S. Mavila, S. Huang, N. Spurgin, J. Sinha, C.N. Bowman, Thiol–Anhydride Dynamic Reversible Networks, Angewandte Chemie International Edition. 59 (2020) 9345–9349. https://doi.org/10.1002/anie.202001388.

[37] M. Delahaye, F. Tanini, J.O. Holloway, J.M. Winne, F.E. Du Prez, Double neighbouring group participation for ultrafast exchange in phthalate monoester networks, Polym. Chem. 11 (2020) 5207–5215. https://doi.org/10.1039/D0PY00681E.

[38] Y. Ecochard, S. Caillol, Hybrid polyhydroxyurethanes: How to overcome limitations and reach cutting edge properties?, European Polymer Journal. 137 (2020) 109915. https://doi.org/10.1016/j.eurpolymj.2020.109915.

[39] A. Bossion, R.H. Aguirresarobe, L. Irusta, D. Taton, H. Cramail, E. Grau, D. Mecerreyes, C. Su, G. Liu, A.J. Müller, H. Sardon, Unexpected Synthesis of Segmented Poly(hydroxyurea–urethane)s from Dicyclic Carbonates and Diamines by Organocatalysis, Macromolecules. 51 (2018) 5556–5566. https://doi.org/10.1021/acs.macromol.8b00731.

[40] N. Fanjul-Mosteirín, C. Jehanno, F. Ruipérez, H. Sardon, A.P. Dove, Rational Study of DBU Salts for the CO_2 Insertion into Epoxides for the Synthesis of Cyclic Carbonates, ACS Sustainable Chem. Eng. 7 (2019) 10633–10640. https://doi.org/10.1021/acssuschemeng.9b01300.

[41] T.M. McGuire, E.M. López-Vidal, G.L. Gregory, A. Buchard, Synthesis of 5- to 8-membered cyclic carbonates from diols and CO2: A one-step, atmospheric pressure and ambient temperature procedure, Journal of CO2 Utilization. 27 (2018) 283–288. https://doi.org/10.1016/j.jcou.2018.08.009.

[42] H.-W. Engels, H.-G. Pirkl, R. Albers, R.W. Albach, J. Krause, A. Hoffmann, H. Casselmann, J. Dormish, Polyurethanes: Versatile Materials and Sustainable Problem Solvers for Today's Challenges, Angew. Chem. Int. Ed. 52 (2013) 9422–9441. https://doi.org/10.1002/anie.201302766.

[43] R.H. Aguirresarobe, S. Nevejans, B. Reck, L. Irusta, H. Sardon, J.M. Asua, N. Ballard, Healable and self-healing polyurethanes using dynamic chemistry, Progress in Polymer Science. 114 (2021) 101362. https://doi.org/10.1016/j.progpolymsci.2021.101362.

[44] B. Jousseaume, C. Laporte, T. Toupance, J.-M. Bernard, Efficient bismuth catalysts for transcarbamoylation, Tetrahedron Letters. 43 (2002) 6305–6307. https://doi.org/10.1016/S0040-4039(02)01391-6.

[45] D.J. Fortman, J.P. Brutman, C.J. Cramer, M.A. Hillmyer, W.R. Dichtel, Mechanically Activated, Catalyst-Free Polyhydroxyurethane Vitrimers, J. Am. Chem. Soc. 137 (2015) 14019–14022. https://doi.org/10.1021/jacs.5b08084.

[46] X. Chen, L. Li, K. Jin, J.M. Torkelson, Reprocessable polyhydroxyurethane networks exhibiting full property recovery and concurrent associative and dissociative dynamic chemistry via transcarbamoylation and reversible cyclic carbonate aminolysis, Polym. Chem. 8 (2017) 6349–6355. https://doi.org/10.1039/C7PY01160A.

[47] X. Chen, L. Li, J.M. Torkelson, Recyclable polymer networks containing hydroxyurethane dynamic cross-links: Tuning morphology, cross-link density, and associated properties with chain extenders, Polymer. 178 (2019) 121604. https://doi.org/10.1016/j.polymer.2019.121604.

[48] X. Chen, L. Li, T. Wei, J.M. Torkelson, Reprocessable Polymer Networks Designed with Hydroxyurethane Dynamic Cross- links: Effect of Backbone Structure on Network Morphology, Phase Segregation, and Property Recovery, Macromol. Chem. Phys. (2019) 1900083. https://doi.org/10.1002/macp.201900083.

[49] X. Chen, L. Li, T. Wei, D.C. Venerus, J.M. Torkelson, Reprocessable Polyhydroxyurethane Network Composites: Effect of Filler Surface Functionality on Cross-link Density Recovery and Stress Relaxation, ACS Appl. Mater. Interfaces. 11 (2019) 2398–2407. https://doi.org/10.1021/acsami.8b19100.

[50] S. Hu, X. Chen, J.M. Torkelson, Biobased Reprocessable Polyhydroxyurethane Networks: Full Recovery of Crosslink Density with Three Concurrent Dynamic Chemistries, ACS Sustainable Chem. Eng. 7 (2019) 10025–10034. https://doi.org/10.1021/acssuschemeng.9b01239.

[51] H. Sardon, A. Pascual, D. Mecerreyes, D. Taton, H. Cramail, J.L. Hedrick, Synthesis of Polyurethanes Using Organocatalysis: A Perspective, Macromolecules. 48 (2015) 3153–3165. https://doi.org/10.1021/acs.macromol.5b00384.

[52] C. Jehanno, M.M. Pérez-Madrigal, J. Demarteau, H. Sardon, A.P. Dove, Organocatalysis for depolymerisation, Polym. Chem. 10 (2019) 172–186. https://doi.org/10.1039/C8PY01284A.

[53] A. Erice, A. Ruiz de Luzuriaga, J.M. Matxain, F. Ruipérez, J.M. Asua, H.-J. Grande, A. Rekondo, Reprocessable and recyclable crosslinked poly(urea-urethane)s based on dynamic amine/urea exchange, Polymer. 145 (2018) 127–136. https://doi.org/10.1016/j.polymer.2018.04.076.

[54] A. Yuen, A. Bossion, E. Gómez-Bengoa, F. Ruipérez, M. Isik, J.L. Hedrick, D. Mecerreyes, Y.Y. Yang, H. Sardon, Room temperature synthesis of non-isocyanate polyurethanes (NIPUs) using highly reactive N-substituted 8-membered cyclic carbonates, Polym. Chem. 7 (2016) 2105–2111. https://doi.org/10.1039/C6PY00264A.

[55] P.J. Flory, Molecular Theory of Rubber Elasticity, Polymer Journal. 17 (1985) 1–12. https://doi.org/10.1295/polymj.17.1.